KINEMATICS MODELING AND SIMULATION ANALYSIS OF VARIABLE CURVATURE KINEMATICS CONTINUUM ROBOTS

Selman DJEFFAL [1, 2], Ammar AMOURI [3,*] and Chawki MAHFOUDI [1, 2]

Continuum robots increasingly attract researchers' interest as long as an accurate solution for their modeling is still outstanding, in particular that having a variable curvature. The key issues in continuum robots are its kinematics models due to: structure complexity, equations nonlinearity, redundancy resolution, and so on. To tackle those issues, the first contribution presented in this paper provides with a methodology to simplify the calculation's complexity of the Forward Kinematics Models (FKMs) of variable curvature continuum robots. The second one presents a numerical solution to their Inverse Kinematics Models (IKMs) by using a powerful optimization method, namely Particle Swarm Optimization (PSO), taking into account specific constraints in both the configuration space and in the Cartesian space. Simulation examples through Matlab software have been carried out to verify and analyze the significance of the proposed contributions approaches. It is noteworthy that the proposed approaches can be successfully applied to constant curvature kinematics continuum robots.

Keywords: Continuum robot, multi-section continuum robot, kinematics modeling, particle swarm optimization, redundancy.

1. Introduction

Traditional rigid robots have shown drawbacks features like restriction in complex environments. To cope with these problems and difficulties, the researchers' ambitions were directed towards creating soft and flexible structures inspired from biological systems found in nature, which are similar to certain appendices and tentacles [1-3]. One-of-many attractive features of these robots, they can easily move in cluttered environments without traditional revolute and prismatic joints, namely they bend and deform continuously along their lengths which makes them suitable for a variety of applications such as search and rescue operations [4], surgical interventions [5-6], underwater operations [7] and so on.

From a modeling point of view, kinematic modeling is considered to be one of the most difficult problems tackled in continuum robots research. However, considerable efforts on the subject have been focused on developing accurate kinematic models with respecting as much as possible some specificities and proprieties of the considered robot. Nevertheless, most of those works, so far,

[1]Department of Mechanical Engineering, University of L'Arbi Ben M'hidi, Oum el Bouaghi, Algeria. E-mail: djeffalselman@gmail.com, mahfoudi.chawki@gmail.com
[2]CMSMTF Laboratory, University of L'Arbi Ben M'hidi, Oum el Bouaghi, Algeria.
[3]Department of Mechanical Engineering, University of Brothers Mentouri, Constantine 1, Algeria. E-mail: ammar_amouri@yahoo.fr

rely on some hypotheses and approximations such as [8-13] in which the common applied hypothesis is the constant curvature (CC) kinematic assumption [8].

Indeed, to have a more realistic behavior of the continuum robot, the variable curvature (VC) kinematic is the closest model which can be adapted. To this end, very few works have been developed [14-17]. In [14], the authors have applied the variable curvature kinematic approach to three pneumatic actuators continuum manipulator. Their kinematic models are strongly related to the constant curvature assumption [8]. The main idea for deriving the FKM is to subdivide each section into virtual units, then use the piecewise constant curvature assumption for each subdivided section. While their IKM is realized as a velocity based-feed forward motion control. In [15-16], both authors propose specific kinematics of a single section based on an energy modeling technique. In [17], the authors have proposed the inverse kinematic problem of a continuum manipulator with a variable curvature. Within the same context, we present in the current paper, a simplified method to calculate the forward kinematic models, and solving its inverse kinematic problem using Particle Swarm Optimization (PSO) method [18]. PSO method is one of heuristic methods which has successfully solved difficult optimization problems in various fields of sciences and engineering [19-20]. The main advantage of this method is its simplicity and fast convergence [21-22]. This method is successfully applied to solve the IKM for a planar and spatial multi-section continuum robot [23-24]. The IKM has been formulated as an optimization problem under the CC assumption.

The main contributions of this paper can be described in two parts; first, the paper presents an approximation solution of the forward kinematic model for a single continuum robot section with variable curvature, assuming that each of its units bends as a circular arc with an inextensible central axis. Then, on the basis of this approximation, the FKM of the multi-section continuum robot has been calculated. The second part, the paper presents a numerical solution to the inverse kinematics models using a heuristic method called Particle Swarm Optimization method and via point-to-point technique.

The rest of the paper is arranged as follows: Section 2 describes the continuum robot design. Section 3 demonstrates the followed methodology to derive the forward kinematic models for variable curvature continuum robot, as well as the identification of its workspace. Section 4 presents the implementation of the PSO method for solving the inverse kinematic models. Section 5 provides with the obtained results on the models validation through a set of numerical simulations. Finally, a conclusion and perspective works conclude this paper.

2. Continuum robot kinematics

In this section, the kinematics description of the variable curvature continuum robot depicted in Fig. 1(a) is briefly presented, whose complex

structure has two conically shaped sections. Each section is mounted at the base of its first conical unit, while the remaining conical units are stacked sequentially on top. Each section has two degrees of freedom, a bending and an orientation angle, and actuated by three independent cables. To have a simplified description of the continuum robot under consideration, the profile of the whole section is assimilated into a curve formed by a serial concatenation of circular arcs, which represents the central axis of it [24], see Fig. 1(b). A detailed illustration of a conically shaped unit showing arc parameters and geometric properties is displayed in Fig. 2. To achieve this purpose, the symbols, variables and parameters shown in Table 1 are used. We note, here, that the index k which refers to the $k-$th section has been omitted in the graphs of Fig. 2.

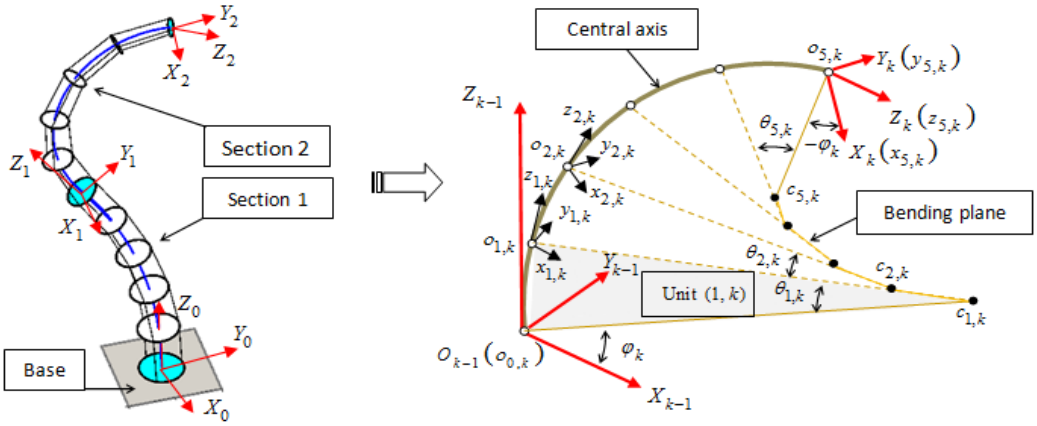

(a) (b)

Fig.1. Continuum robot kinematics: (a) global coordinate frames for each section k, (b) local Coordinate frames of each unit (j,k).

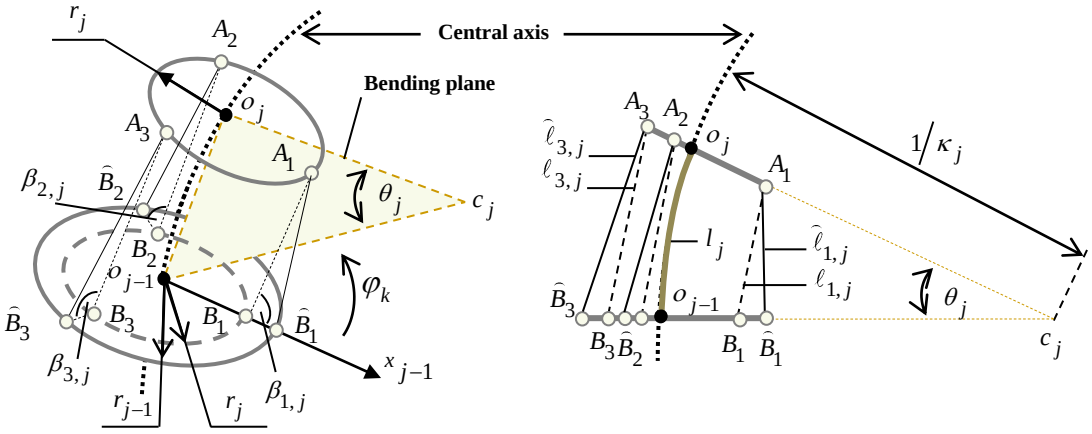

Fig. 2. Geometry of a single conically shaped unit (j,k) and its kinematics nomenclature

Table 1

Kinematics nomenclature

i	: is the index of cables $i = 1, 2, 3$	$(x, y, z)_{j,k}$	: is the local coordinate frame
j	: is the index of units $j = 1, 2, ..., m$	$(X, Y, Z)_k$	: is the global coordinate frame
k	: is the index of sections $k = 1, 2$	$\theta_{j,k}$	: is the bending angle
$\ell_{i,j}$	: is the non-conic unit cable length	φ_k	: is the orientation angle
$\widehat{\ell}_{i,j}$	: is the conic unit cable length	κ_j	: is the curvature
l_j	: is the length of the central axis of the unit j	r_j	: is the radial distance between cables and the central axis

3. Forward Kinematics Modeling

In this section, we describe the simplified methodology which derives the forward kinematic modeling of variable curvature continuum robot; it mainly depends on the constant curvature assumption [8] and relates to the following assumptions:

i. The continuum robot is described as an open kinematic chain of sections;
ii. Each section is a set of equally-spaced concatenation with a number of conically shaped units and their cables lengths are homogeneously fragmented.
iii. Each section bends without torsion effect;
iv. Each conically shaped unit is modeled as an inextensible arc of circle having its individual arc parameters and bends in weak angles.

According to those assumptions, the relationships from the actuator space to the Cartesian space, i.e. the FKMs, for the continuum robot can be derived through three steps. Starting with the FKM of a single conically shaped unit, then the FKM of a single section and finally, the FKM of a multi-section continuum robot.

3.1. FKM of a single conically shaped unit

As shown in Fig. 2, a single conical unit of the continuum robot is considered when it comes to calculating the forward kinematic model. In general, this model consists in representing the operational coordinates $\mathbf{X}_{j,k}$ as a function of the cables length $\widehat{\mathbf{Q}}_{j,k}$ through arc parameters $\mathbf{K}_{j,k}$ (see Fig. 3). Therefore, under the assumption that each unit bends as a circular arc shape, the independent transformation can be written as Equation (1) [8]. For simplicity reasons, we note that the index k which refers to the $k-$th section will be omitted in the following formulation.

$$ {}^{j-1}\mathrm{T}_j = \begin{bmatrix} {}^{j-1}\mathrm{R}_j & {}^{j-1}\mathrm{P}_j \\ 0_{1\times 3} & 1 \end{bmatrix} \tag{1} $$

with

$$ {}^{j-1}\mathrm{R}_j = \mathrm{rot}_{z_{j-1},\varphi_k} \cdot \mathrm{rot}_{y_{j-1},\theta_j} \cdot \mathrm{rot}_{z_{j-1},-\varphi_k} \tag{2} $$

$$ {}^{j-1}\mathrm{P}_j = \begin{cases} \dfrac{l_j}{\theta_j}\left(1-\cos\left(\theta_j\right)\right)\cos\left(\varphi_k\right) \\ \dfrac{l_j}{\theta_j}\left(1-\cos\left(\theta_j\right)\right)\sin\left(\varphi_k\right) \\ \dfrac{l_j}{\theta_j}\sin\left(\theta_j\right) \end{cases} \tag{3} $$

where ${}^{j-1}\mathrm{R}_j$ is the orientation matrix of frame $\Re_j\left(o_j, x_j, y_j, z_j\right)$ with respect to $\Re_{j-1}$, and ${}^{j-1}\mathrm{P}_j$ is the position vector which defines o_j in frame $\Re_{j-1}$.

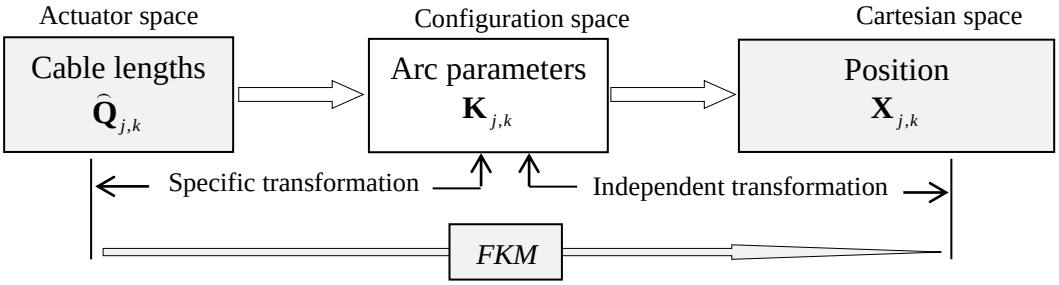

Fig.3. Global view of the single unit modeling

The specific transformation that expresses the cables length, $\ell_{i,j}$, of each cylindrically shaped unit as a function of arc parameters can be written as [8]

$$ \theta_j = \frac{2\sqrt{\ell_{1,j}^2 + \ell_{2,j}^2 + \ell_{3,j}^2 - \ell_{1,j}\ell_{2,j} - \ell_{1,j}\ell_{3,j} - \ell_{2,j}\ell_{3,j}}}{3r_j} \tag{4} $$

$$ \varphi_k = \tan^{-1}\left(\frac{\sqrt{3}\left(\ell_{3,j} - \ell_{2,j}\right)}{2\ell_{1,j} - \ell_{2,j} - \ell_{3,j}}\right) \tag{5} $$

where r_j is the distance between the center of the unit $\left(j,k\right)$ and the location of each driving cable which can be expressed as

$$r_j = r_{\max,k} - \frac{j}{m}\left(r_{\max,k} - r_{\min,k}\right) \tag{6}$$

where $r_{\min,k}$ and $r_{\max,k}$ are, respectively, the minimum and the maximum radius of the section *k*. The values of those parameters are given in Table 2.

Table 2

Parameters of the considered continuum robot

	Section $k=1$	Section $k=2$	Description
m_k	5 units	5 units	Number of physical units per section
L_k	300 mm	300 mm	Total length of the section
$r_{\min,k}$	17.5 mm	10 mm	Radial cable distance
$r_{\max,k}$	25 mm	17.5 mm	Radial cable distance

As long as each unit has a conically shaped form, Equations (4) and (5) should be expressed depending on the cable lengths $\widehat{\ell}_{i,j}$ instead of $\ell_{i,j}$. Therefore, according to the assumption (iv), we use the analytical approximation solution proposed in [14], as

$$\ell_{i,j} = \sqrt{\widehat{\ell}_{i,j}^2 - \left(r_j - r_{j-1}\right)^2} \tag{7}$$

3.2. FKM of a single continuum robot section

According to assumption (ii) and (iii), the FKM of a single continuum robot section can be expressed as

$${}^{k-1}\mathrm{T}_k = \prod_{j=1}^{m} {}^{j-1,k}\mathrm{T}_{j,k} \tag{8}$$

where ${}^{j-1,k}\mathrm{T}_{j,k}$ is the homogenous transformation matrix defines the position and orientation of the platform unit's frame $\Re_j$ with respect to its base frame $\Re_{j-1}$.

On the other hand, the continuum robot section is equally subdivided into m units with weak bending angles, which leads to an important observation, namely a constant ratio which relates arc parameters and geometric parameters of the section's units. Thus, we can get the following relationship as

$$\theta_{j,k} = \frac{r_{1,k}}{r_{j,k}}\theta_{1,k} \tag{9}$$

Remarkably, an increased number of units, increases also the accuracy of solutions from the equation (9) (i.e. the angle β_i is closer to $\pi/2$, see Fig. 2). Therefore, by using the Equation (9), the FKM of a single section can be only expressed by two variables $\theta_{1,k}$ and φ_k. This approximation leads to a remarkable

simplification and reduction in the number of variables involved in the FKM as well as the calculation of the IKM. Considering the previously made simplification, the FKM and IKM will be accordingly developed in the following sections. An illustration of Equation (9) is shown in Fig. 4. The left side of this Figure illustrates the plot of different bending angles as a function of a given variation in cables length of each unit. The constant ratios relate arc parameters and geometric parameters are illustrated in the right side of Fig. 4.

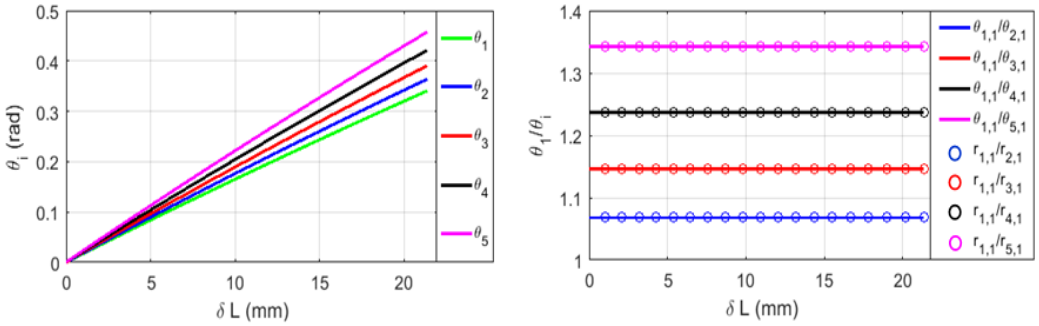

(a) (b)

Fig.4. (a) Bending angles as a function of a given variation in cables length for each unit, (b) The constant ratios relate arc parameters and geometric parameters of the section $\left(k=1\right)$

3.3. FKM of multi-section continuum robot

According to assumption (i), the FKM of the multi-section continuum robot can be easily established using the previous homogeneous transformations as

$$^{0}\mathrm{T}_{n}=\prod_{k=1}^{n=2}{}^{k-1}\mathrm{T}_{k} \tag{10}$$

where $^{k-1}\mathrm{T}_{k}$ represents the transformation matrix of frames from platform k to platform $k-1$, and it is associated with the $k-$th section of the continuum robot.

3.4. Workspaces generation

In order to generate the desired trajectory that the robot can properly track, its workspace must be known. It presents the set of all reachable positions by the robot's tip. For simplicity reasons, Fig. 5 shows the possible end-positions of the first section and of the continuum robot in two dimensional representations. These points were obtained using the FKM for the first bending angle of each section which ranges as $\theta_{1,k}\in[-\pi/8,\ \pi/8]$. In this Figure, some possible positions that the continuum robot's tip can reach are denoted by the letter A (red, dotted curved-lines), and the reachable positions by the robot's first section are denoted by the letter B (yellow, dotted curved-lines). To thoroughly understand the behavior of

the considered robot within its workspace, we fixed the robot's first section in specific positions and exclusively allowed the robot's second section to move, it's possible movements is illustrated by the letter C (black, solid curved-lines) , three black curved-lines for each specified position.

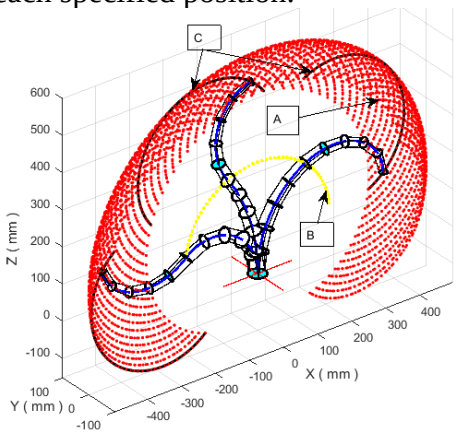

Fig.5. 2D view of the workspace for the continuum robot with two sections and reachable positions for each section.

4. PSO based approach for solving inverse kinematics models

For any robotic system, the inverse kinematics model can be summarized as: for a given posture, position and orientation, find the needed actuator vector variables which satisfy some motions constraints. To achieve this purpose, various methods were explored based on the forward kinematics models such as the works in [8, 14, 17, 25]. But due to the nonlinearity of the forward kinematic model and the kinematic redundancy of this kind of robots, it is generally very difficult to solve this problem directly. Even, if the set of nonlinear equations can be solved, the unique solution is not guaranteed. Usually, these problems are addressed using an algorithm which minimizes/maximizes a set of given criteria [23-25]. In this context, a powerful optimization method namely, Particle Swarm Optimization, is implemented to choose one inverse kinematic solution among an infinite number of configurations satisfying a certain additional constraints.

4.1. Particle Swarm Optimization

PSO is a population-based search algorithm, developed by Kennedy and Eberhart [18]. This method is based on the simulation of the social behavior of a set of birds, fishes and other flocks.

In the PSO algorithm, the starting phase consists of randomly generated particles which aim at reaching optimal solutions through updating iterations. At each iteration step t, four available information for each particle p: the first information is the local position vector of the best solution which was achieved so

far and is denoted by $P_b(t)$. The second one is the position visited by the particle swarm optimizer which is selected by all particles' best experiences, it represents the global best position and denoted by $P_{gb}(t)$. Other information is the current position of a particle in search space given by a vector $P(t)$ and its velocity given by $\mathrm{v}(t)$. Therefore, velocities and positions of particles keep changing at each step time t until they are suitable according to the following equations:

$$\mathrm{v}(t+1) = \omega \mathrm{v}(t) + \mathrm{c}_1\lambda_1\left(P_b(t) - P(t)\right) + \mathrm{c}_2\lambda_2\left(P_{gb}(t) - P(t)\right) \tag{11}$$

$$P(t+1) = P(t) + \mathrm{v}(t+1) \tag{12}$$

where ω is the inertia weight; c_1, c_2 are two positive constants; and λ_1, λ_2 are two random numbers with uniform distribution between 0 and 1.

The importance of parameters involved in equation (11) is to provide the algorithm behavior with the needed convergence. For instance, the inertia ω gives the algorithm's convergence rate, in some challenging problems, rate is required to be applied in small increments in order to keep the algorithm stable, and the coefficients c_1 and c_2 guide the tendency of the swarm to converge to a local or global best solution. Basically, iterations number and swarm size mainly depend on the complexity of the studied optimization problem.

4.2. The objective function and Problem setting

When via point's technique is concerned in robots tracking trajectory, the robot's tip requires specific actuator vector variables to properly track the described and desired trajectory. Additionally, the orientation robot's tip cannot be ensured for the considered multi-section continuum robot. Due to these challenging conditions, an appropriate objective function is proposed to be an alternative solution and which can be expressed as

$$f_{obj} = \left|\mathbf{X}_d - \mathrm{X}_g\right| \tag{13}$$

where $\mathbf{X}_d$ and X_g are, respectively, the desired and the generated Cartesian coordinates of the continuum robot's tip given by the fourth column of the homogeneous matrix defined in Equation (10).

On the other hand, due to the continuum robot's hyper-redundancy, equation (13) has an infinite number of solutions. Therefore, to select one solution among them, additional constraints are added to the objective function, which are discussed in the simulations analysis section.

The main purpose of this section is to find the bending and orientation angles (i.e. $\theta_{1,k}$ and φ_k) of each section, which will be adopted to make the robot's tip track the desired trajectory via point-to-point technique. To this end, at each sampling instant, the optimization problem, Equation (13), has been solved

to obtain the sequences $\theta_{1,k}$ and φ_k, in which the last sequence is considered to be the optimized couples applied to the robot. In this case, the coordinates of the particle in PSO are the variables of the optimization problem and the particle swarm is the set of possible solutions of the problem.

5. Simulations analysis

To underline the efficiency of the proposed forward and inverse kinematics solutions, three simulation examples for tracking trajectory via point-to-point technique are considered. The first is related to a single section. The second example concerns a continuum robot with two sections in the planar projection; while the last one is considered for the three-dimensional case. The geometric parameters describing the multi-section continuum robot in this study are presented in Table 2. The implementing process has been performed in Matlab software using an Intel Core i3, 2.10 GHz, 4 GB RAM.

5.1. Simulation one

In this simulation, the continuum robot with five units corresponding to the first section is parameterized in Table 2, as depicted in Fig. 6, is used for tracking a trajectory on its own workspace. In this simulation example, we only considered the configuration and Cartesian spaces; thus, for a given Cartesian coordinates of the section's tip, the variation of bending and orientation angles have been calculated and saved, using the proposed IKM. On the other hand, in order to verify the efficiency of the proposed model, the corresponding bending and orientation angles are calculated using FKM. Figure 7 shows the bending and orientation angles calculated by the FKM and those obtained by PSO method, i.e. IKM, where the Euclidean errors are deduced. It can be seen that there is a significant convergence between them, where the maximum error is less than 0.0008 rad.

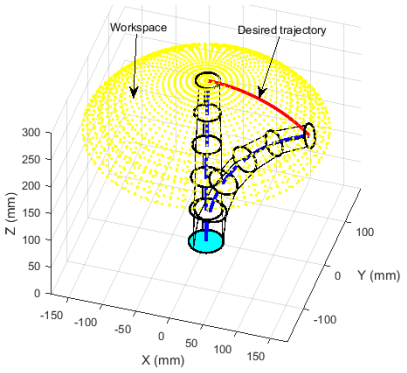

Fig. 6. Representation of the initial and final configuration of the continuum robot's first section tracking the desired trajectory in its own 3D workspace

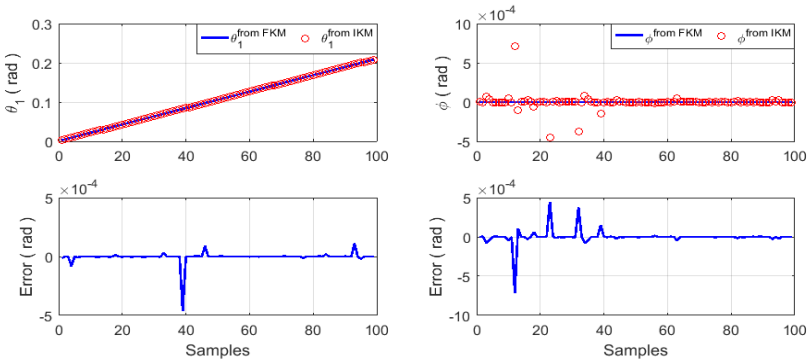

Fig. 7. Bending and orientation angles obtained from FKM and IKM

5.2. Simulation two

In the second simulation, the continuum robot with two sections, each section consists of five units, is considered to track the trajectory which is defined by Equation (14). Figure 8(a) shows some solutions of IKM, i.e. possible configurations of the robot, for a given point of the desired trajectory. Due to the robot's redundancy, for instance, in order to select one solution among the infinite ones, the additional constraints defined as $\theta_2 > 0$ and $0 < \varphi_1, \varphi_2 < 10^{-5}$ have been added to the objective function. Figure 8(b) presents some configurations of the robot for the desired tracking trajectory with previously-defined additional constraints, and the corresponding profile of cables length is presented in Fig. 9.

$$\begin{cases} X_2 = 10t \\ Y_2 = 30 \quad \text{, for } t = 0:0.5:35 \\ Z_2 = 400 \end{cases} \tag{14}$$

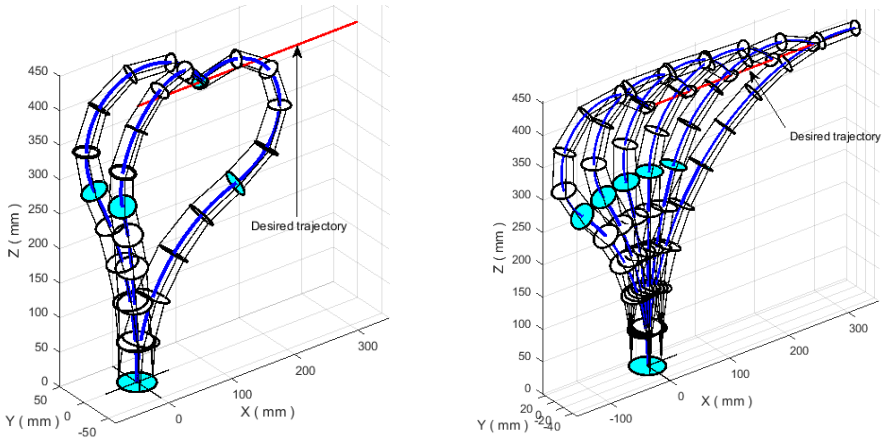

(a) (b)

Fig. 8. Continuum robot's configuration, (a) Possible solutions for each desired point, (b) Some configuration of the robot tracking the desired trajectory with additional constraints.

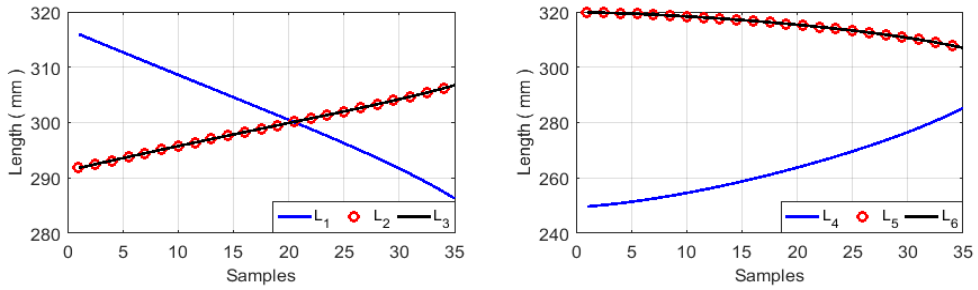

Fig. 9. Calculated cables length

Because the calculation of the cables length is strongly related to the proposed approximation (Equation (9)), the effect of the latter is clearly visible on the profile of the cables length of each unit, as shown in Fig. 10 and 11. It is obviously clear that the more the bending of a section increases, the more the cables' length of each unit orderly decrease from bottom to top. To thoroughly point out this phenomenon, we can refer to the second section, where the robot enormously bends, in particular the last position. From these observations, we can say that the six cables' length converge to the last point as shown in Fig. 11.

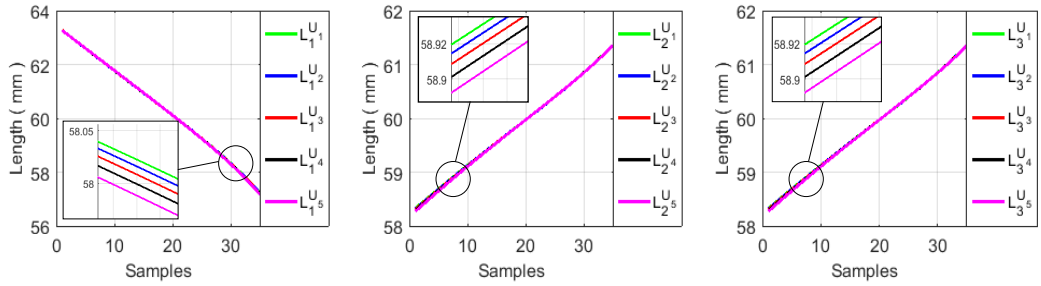

Fig. 10. Profile of the cables length for the first section's units.

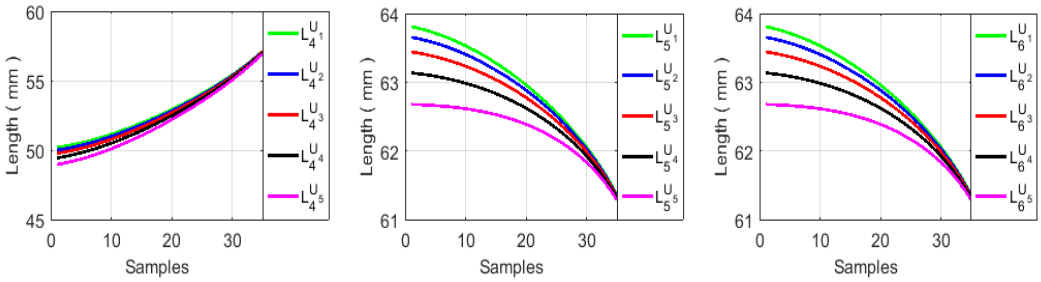

Fig. 11. Profile of the cables length for the second section's units.

5.3. Simulation three

Similar to the second simulation, the same robot tracks a circular spatial trajectory defined by Equation (15). To select one IK solution, the additional

constraints defined as $\theta_{1,1} < 0$, $\theta_{1,2} > 0$ and $0 < Y_1 < 10^{-6}$ are added to the objective function.

$$\begin{cases} X_2 = 30\cos(\pi t/5) \\ Y_2 = 30\sin(\pi t/5) \\ Z_2 = 440 + 30\sin(\pi t/5) \end{cases}, \text{for } t = 1:0.25:10 \tag{15}$$

The illustration of this example is shown in the left side of Fig. 12. The right side of this Figure shows the desired and the generated trajectory by the proposed model, where the Euclidean errors are deduced (see the bottom side of Fig. 12(b)). The profile of cables length which allows the robot to track the trajectory is shown in Fig. 13. For each section, the first bending and orientation angles are shown in Fig. 14.

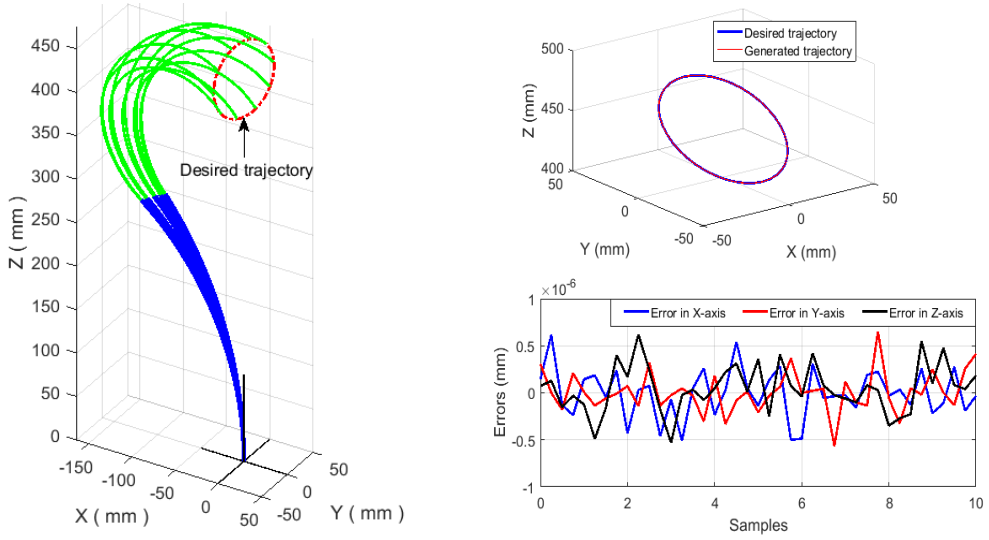

(a) (b)

Fig.12. (a) Some configurations of central axis of the robot tracking the desired circular trajectory, (b) Trajectory comparison with reference and their Euclidean errors

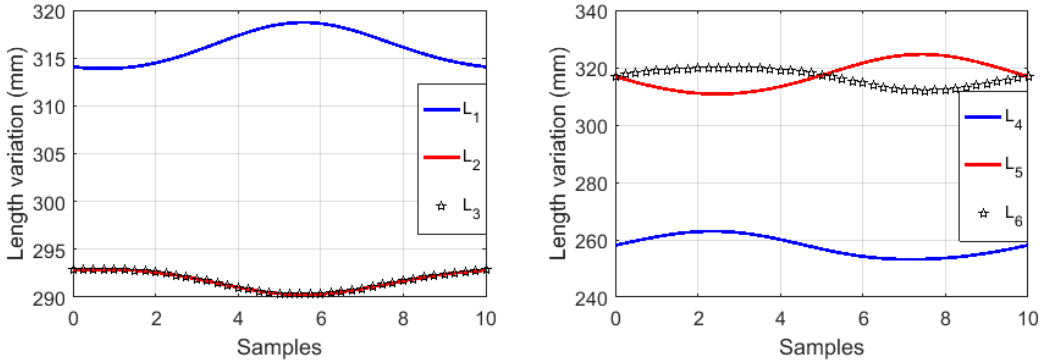

Fig.13. Profile of cables length

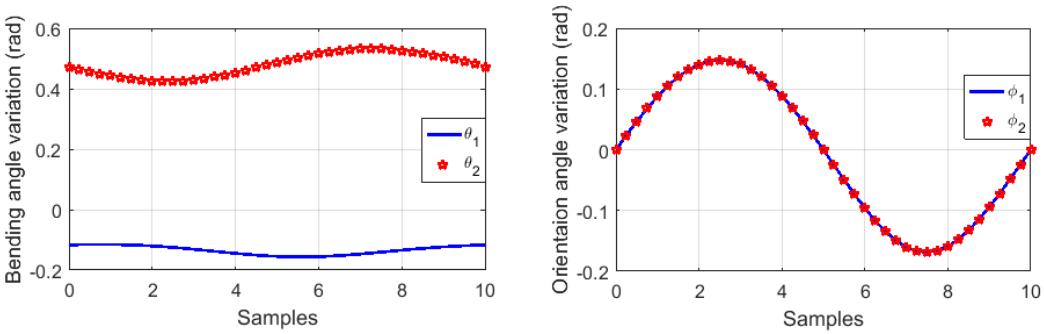

Fig.14. Bending and orientation angles

To sum it up, the adopted approximation which is described by equation (9) significantly facilitates the implementation of FKM, namely few variables are included to develop its theory. Additionally, the Proposed FKM is able to accurately predict the continuum robot's tip in particular for the case of weak bending angles, while the positioning errors of the IKM depends on the desired precision and the time execution of PSO method. In the view of the obtained results, the proposed kinematic models are satisfying and achieve good performance.

6. Conclusion

In this paper, we presented a methodology to calculate the forward kinematic modeling of variable curvature continuum robots, and solving its inverse kinematic problem. The proposed modeling approaches are able to model hyper-redundant or continuum robots that consist of multi-section. The advantage of the proposed approach serves to narrow down the number of variables which appear when calculating the FKM of multi-section continuum robot with variable curvature, in other words, the complexity of the non-linearity of its governing equations can be simplified through the proposed methodology. On the other hand, the inverse kinematic modeling of continuum robots is mathematically

solved through the governing objective function. To make sure that the proposed modeling approaches are efficient, various simulations examples are dedicated to tracking different types of trajectory. In the view of the obtained results, the proposed FKM and IKM have shown their suitability for use in continuum robot as well as achieving good performance. In addition, they are reliably able to model continuum robots with more than two sections. And more importantly, the proposed approaches show a significant accuracy even for weak bending angles of continuum robots which permits to skillfully control continuum robots in different operations. From a practical point of view, the studied robot in this paper is undoubtedly not a straightforward mechanism, since some of the adopted assumptions are difficult to implement; for instance, its cables lengths are homogeneously fragmented which requires an elaborate means to satisfy this condition, yet its practical realization is doable and of an interest. Since the PSO method does not depend on the degree of redundancy of the robot and its characteristics; therefore, a possible extension of the proposed approaches to continuum robots with variables elongation will be addressed in future works.

R E F E R E N C E S

[1]. *D. Trivedi, C. D. Rahn, W. M. Kier, et al.*, "Soft robotics: biological inspiration, state of the art, and future research", Applied Bionics and Biomechanics, **vol. 5**, no. 3, 2008, pp. 99–117.

[2]. *G. Robinson, J. B. C. Davies*, "Continuum robots – a state of the art," In Proceedings of IEEE International Conference on Robotics and Automation, Detroit, Michigan, 1999, pp. 2849–2854.

[3]. *I. Walker*, "Continuous Backbone 'Continuum' Robot Manipulators," ISRN Robotics. 2013.10.5402/2013/726506.

[4]. *H. Tsukagoshi, A. Kitagawa, M. Segawa*, "Active hose: an artificial Elephant's nose with maneuverability for rescue operation," In Proceedings of IEEE International Conference on Robotics and Automation, Seoul, Korea, 2001, pp. 2454–2459.

[5]. *N. Simaan, R. Taylor, P. Flint*, "A dexterous system for laryngeal surgery," In Proceedings of IEEE International Conference on Robotics and Automation, 2004, pp. 351–357.

[6]. *S. Wakimoto, K. Suzumori*, "Fabrication and basic experiments of pneumatic multi-chamber rubber tube actuator for assisting colonoscope insertion," In Proceedings of IEEE International Conference on Robotics and Automation, Anchorage, AK, 2010, pp. 3260–3265.

[7]. *V. C. Anderson, R. C. Horn*, "Tensor arm manipulator design," ASME Transactions, **vol**. **57**, no 2, 1967, pp. 1–12.

[8]. *R. J. Webster, B. A. Jones*, "Design and kinematic modeling of constant curvature continuum robots: A review," International Journal of Robotics Research, **vol. 29**, no. 13, 2010, pp. 1661–1683.

[9]. *S. Mosqueda, Y. Moncada, C. Murrugarra, et al.*, "Constant curvature kinematic model analysis and experimental validation for tendon driven continuum manipulators," In Proceedings of the 15th International Conference on Informatics in Control, Automation and Robotics, **vol. 2**, 2018, pp. 211–218.

[10]. *A. Amouri*, "Investigation of the constant curvature kinematic assumption of a 2-Dofs cable-driven continuum robot," UPB Scientific Bulletin, Series D: Mechanical Engineering, **vol. 81**, 2019, pp. 27–38.

[11]. *B. A. Jones, I. D. Walker*, "Kinematics for multi-section continuum robots," IEEE Transactions on Robotics, **vol. 22**, no. 1, 2006, pp. 43–55.
[12]. *M. W. Hannan, I. D. Walker*, "Kinematics and the implementation of an elephant's trunk manipulator and other continuum style robots," Journal of Robotic Systems, **vol. 20**, no. 2, 2003, pp. 45–63.
[13]. *R. Matthias, J. S. Jochen*, "Constant curvature continuum kinematics as fast approximate model for the Bionic Handling Assistant," In Proceedings of International Conference on Intelligent Robots and Systems, Vilamoura, Algarve, Portugal, 2012. pp. 3440–3446
[14]. *T. Mahl, A. Hildebrandt, O. Sawodny*, "A variable curvature continuum kinematics for kinematic control of the bionic handling assistant," IEEE Transactions on Robotics, **vol. 30**, no.1, 2014, pp. 935–949.
[15]. *D. Trivedi, A. Lotfi, C. Rahn*, "Geometrically exact models for soft robotic manipulators," IEEE Transactions on Robotics, **vol. 24**, no. 4, 2008, pp. 773–780.
[16]. *J. S. Kim, G. S. Chirikjian*, "Conformational analysis of stiff chiral polymers with end-constraints," Journal of Molecular Simulation, **vol. 32**, 2006, pp. 1139–1154.
[17]. *M. Giorelli, F. Renda, G. Ferri, et al*., "A feed-forward neural network learning the inverse kinematics of a soft cable-driven manipulator moving in three-dimensional space," In the Proceedings of IEEE International Conference on Robotics and Automation, 2013, pp. 5033–5039.
[18]. *J. Kennedy, RC. Eberhart*, "Particle swarm optimization," In the Proceedings of IEEE International Conference on Neural Networks IV, 1995, pp. 1942–1948.
[19]. *R. C. Eberhart and Y. Shi* , "Particle swarm optimization: developments, applications and resources," In Proceedings of the Congress on Evolutionary Computation Seoul, Korea, 2001.
[20]. *M. N. K., Kulkarni, M. S., Patekar, M. T., Bhoskar, et al.,* "Particle Swarm Optimization Applications to Mechanical Engineering- A Review," Materials Today: Proceedings, **vol. 2**, no 4–5, 2015, pp. 2631–2639.
[21]. *A. Lazinica,* "Particle Swarm Optimization," 2009, ISBN: 978-953-7619-48-0, Publisher: InTech, Available from: http://www.intechopen.com/books/particle swarm optimization.
[22]. *A. R. Jordehi and J. Jasni*, "Parameter selection in particle swarm optimization: A survey" Journal of experimental and theoretical artificial intelligence, **vol. 25**, no. 4, 2013, pp. 527–542.
[23]. *A. Amouri, C. Mahfoudi, A. Zaatri, et al*., "A new approach to solve inverse kinematics of flexible continuum planar robot," AIP Conference Proceedings, 2014, pp. 643–646.
[24]. *A. Amouri, C. Mahfoudi, A. Zaatri, et al.*, "A metaheuristic approach to solve inverse kinematics of continuum manipulators, " Journal of systems and Control Engineering, **vol. 231**, no. 5, 2017, pp. 380–394.
[25]. *O. Lakhal, A. Melingui, A. Chibani, et al.* "Inverse kinematic modeling of a class of continuum bionic handling arm," In the Proceedings of ASME/IEEE International Conference on Advanced Intelligent Mechatronics, Besançon, France, 8–11 July 2014, pp. 1337–1342.